INSTITUTE OF PHYSICS PUBLISHING SUPERCONDUCTOR SCIENCE AND TECHNOLOGY

Supercond. Sci. Technol. **18** (2005) 798–804 doi:10.1088/0953-2048/18/6/002

Study of the crystal structure, superconducting and magnetic properties of $Ru_{1-x}Fe_xSr_2GdCu_2O_8$

R Escamilla[1], F Morales[1], T Akachi[1] and R Gómez[2]

[1] Instituto de Investigaciones en Materiales, Universidad Nacional Autónoma de México, CU, Apartado Postal 70-360, México DF 04510, Mexico
[2] Facultad de Ciencias, Universidad Nacional Autónoma de México, CU Circuito Exterior, México DF 04510, Mexico

Received 12 November 2004, in final form 1 April 2005
Published 25 April 2005
Online at stacks.iop.org/SUST/18/798

Abstract
Samples from the $Ru_{1-x}Fe_xSr_2GdCu_2O_8$ system with $x = 0$, 0.025, 0.05, 0.075, 0.1 and 0.2, were prepared and their structural, superconducting and magnetic properties were studied. Rietveld refinement of the x-ray diffraction patterns shows that the Fe substitution occurs at both Ru and Cu sites. An increase of Fe concentration produces no significant changes in the Ru–O(3)–Ru bond angle, which is a measure of the rotation of the RuO_6 octahedra around the c-axis, or in the Cu–O(1)–Ru bond angle ϕ, which is a measure of the canting of the RuO_6 octahedra. On the other hand, the Cu–O(2)–Cu bond angle, which is a measure of the buckling of the CuO_2 layer, has a slight tendency to decrease with increase of the Fe content. We found that both ferromagnetic and superconducting transition temperatures are reduced with increase of the Fe concentration. Analysis related to the decay of the superconducting and ferromagnetic states is presented.

1. Introduction

The discovery of the coexistence of superconductivity and ferromagnetism in the ruthenocuprate compound $RuSr_2GdCu_2O_8$ (Ru-1212) [1–5] has raised considerable interest in understanding the intrinsic properties of this layered material. The tetragonal crystal structure of the Ru-1212 compound can be described on the basis of the similarity to $REBa_2Cu_3O_{7-\delta}$ (RE-123) superconductors. The structure of Ru-1212 contains two CuO_2 layers separated by a single oxygen-free Gd layer, the RuO_2 layer replacing the CuO chains present in RE-123 superconductors and a SrO layer located between the CuO_2 and RuO_2 layers. The superconductivity is associated with the CuO_2 layers, as in the RE-123 superconductors, while the ferromagnetism seems to be induced in the RuO_2 layers. The ferromagnetic transition temperature, T_M, is about 135 K, while the superconducting transition temperature, T_c, occurs in the 0–45 K range, depending on sample preparation procedure [6, 7]. Zero-field muon spin rotation measurements [3] and other experiments have shown [8, 9] that the Ru-1212 compound is microscopically uniform with no evidence for spatial phase separation of superconducting and magnetic regions, indicating the three-dimensional character of superconductivity and a uniform long-range magnetic order. Neutron diffraction experiments [10, 11] have demonstrated that the Ru sublattice shows a G-type antiferromagnetic structure, with an ordering moment of the order of 1 μ_B. From magnetization measurements a ferromagnetic ordering has been observed and it was proposed that the origin of the ferromagnetic moment is the canting of Ru moments that give a net moment perpendicular to the c-axis [11, 12]. However, how a ferromagnetic component emerges from an antiferromagnetic background is still unclear.

Several studies of cation substitutions in the Ru-1212 compound have been reported in the literature [13–20]. Their effects on the superconducting and magnetic properties depend on the type of cation and the substitutional site. Studies on the $Ru_{1-x}Sn_x$-1212 system [13, 14] show that the Sn doping suppresses the ferromagnetic moment in the RuO_2 layer, decreasing T_M, but, on the other hand, T_c increases with increase of the Sn content. These results were attributed to

 © 2005 IOP Publishing Ltd Printed in the UK

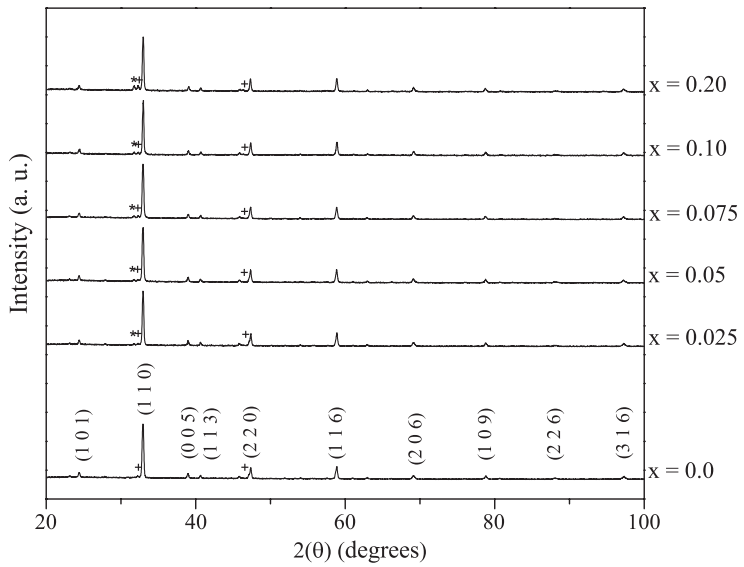

Figure 1. X-ray diffraction patterns for the $Ru_{1-x}Fe_xSr_2GdCu_2O_8$ samples. The symbols + and * indicate peaks of $SrRuO_3$ and $Sr_3(Ru, Cu)O_7$ impurity phases, respectively.

the diamagnetic properties of Sn ions that reduce the total magnetic moment in the RuO_2 layers and increase the hole transfer to the CuO_2 layers. Substitutions in Ru sites with Ti [15, 16], Nb [15], Rh [16] and Co [17] have shown that both T_M and T_c decrease with increasing doping. A peculiar behaviour of enhancement of both T_M and T_c has been found for V substitution at Ru sites [15]. This behaviour could be attributed to the ability of vanadium to adopt a 4+/5+ mixed valence. Klamut *et al* [18] have investigated Cu substitutions at Ru sites. They found that T_c values strongly increase with doping, reaching a maximum of 72 K, and when Ru is replaced by Cu up to 20 at.%, they detected signals of magnetic ordering, above the superconducting transition temperatures, but no ferromagnetic signals of the Ru sublattice were detected at higher doping levels. They also observed a re-entrant magnetization below T_c due to the paramagnetic response of the Gd sublattice. Studies of La substitution at Sr sites [19] have been performed and the results show that T_M increases slightly, but the superconductivity is strongly reduced by doping, due to a hole trapping mechanism caused by disorder defects. Substitution of Zn at Cu sites [20], as in other high-T_c cuprate superconductors, rapidly suppresses the superconductivity due to pair breaking mechanisms.

Although there is general agreement that in $RuSr_2GdCu_2O_8$ the superconductivity originates in the CuO_2 layers and the ferromagnetism in the RuO_2 layers, further understanding is required to have knowledge about the nature of this ferromagnetic superconductor. With this objective in mind, we performed Fe doping experiments, investigating the possible influence of the iron magnetic moment on the magnetic and superconducting properties of the Ru-1212 compound. Thus, in this paper we report our results related to the structural properties, the electrical resistivity and the magnetic properties of the $Ru_{1-x}Fe_xSr_2GdCu_2O_8$ system as a function of Fe doping, temperature and external magnetic field.

2. Experimental details

Polycrystalline samples of $Ru_{1-x}Fe_xSr_2GdCu_2O_8$ ($Ru_{1-x}Fe_x$-1212), with $x = 0$, 0.025, 0.05, 0.075, 0.1 and 0.2, were synthesized by solid state reaction of stoichiometric quantities of the oxides RuO_2 (99%), Fe_2O_3 (99.999%), Gd_2O_3 (99.9%), CuO (99.99%) and $SrCO_3$ (98+%). After calcination in air at 900 °C, the material was ground, pressed into pellets and annealed in oxygen atmosphere at 1000 °C for 72 h. Phase identification of the samples was done with an x-ray diffractometer Siemens D5000 using Cu Kα radiation and a Ni filter. Intensities were measured at room temperature in steps of 0.02°, for 14 s, in the 2θ range 20°–100°. The crystallographic phases were identified by comparison with the x-ray patterns of the JCPDS database. The crystallographic parameters were refined using a Rietveld refinement program, Rietica v 1.7.7 [21], with multi-phase capability. The superconducting transition temperatures were determined in a closed-cycle helium refrigerator by measuring resistance versus temperature. The resistance was measured by the four-probe technique in the temperature range of 14–250 K. dc magnetization measurements were performed in a superconducting quantum interference device (SQUID) based magnetometer, in the temperature range of 2–300 K.

3. Results and discussion

Figure 1 shows the x-ray diffraction patterns for the synthesized samples of $Ru_{1-x}Fe_x$-1212. The analysis of these data indicates that the crystal structure of the samples corresponds to that of Ru-1212 structure, although for $x = 0$ faint features of the $SrRuO_3$ structure (ICDD No 41-1442) were observed and additional peaks corresponding to the $Sr_3(Ru, Cu)_2O_7$ (ICDD No 51-0307) phase were also detected for $x \geqslant 0.025$. The x-ray diffraction patterns of the samples were Rietveld fitted using space group $P4/mmm$ (No 123), taking into account the possibility that Fe can also occupy Cu sites and the presence

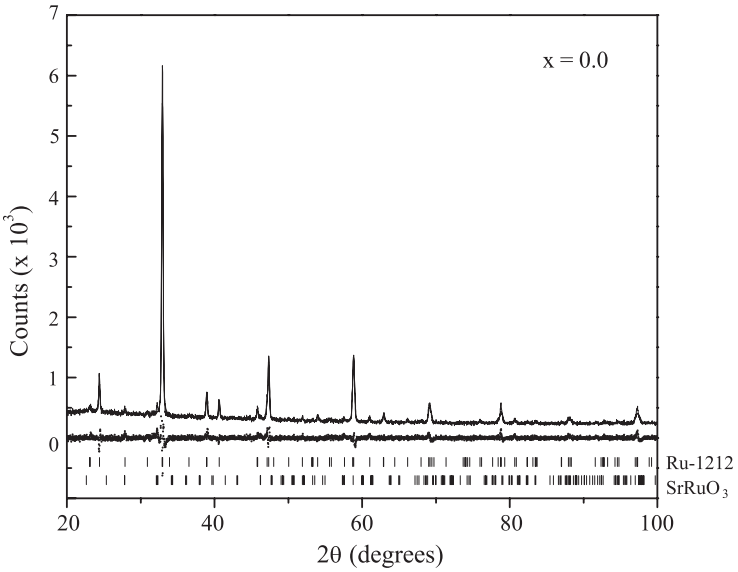

Figure 2. Rietveld refinement of the x-ray diffraction pattern for the $x = 0.0$ sample. Experimental spectrum (dots), calculated pattern (continuous line), their difference (middle line) and the calculated peak positions (bottom).

Table 1. Structural parameters for $Ru_{1-x}Fe_x$-1212 at 295 K. Space group: $P4/mmm$ (No 123). Atomic positions: Ru: 1b (0, 0, 1/2); Gd: 1c (1/2, 1/2, 0); Sr: 2h (1/2, 1/2, z); Cu: 2g (0, 0, z); 2O(1) at 8s (x, 0, z) × 1/4, 4 O(2) at 4i (0, 1/2, z), and 2O(3) at 4o (x, 1/2, 1/2) × 1/2 position. N (Fe) is the iron occupancy parameter.

	x	0.0	0.025	0.05	0.075	0.10	0.2
	a (Å)	3.8369(3)	3.8373(2)	3.8385(2)	3.8393(4)	3.8395(4)	3.8412(4)
	c (Å)	11.563(3)	11.557(2)	11.555(3)	11.542(3)	11.539(4)	11.528(4)
	V (Å^3)	170.23(3)	170.18(2)	170.25(2)	170.13(4)	170.11(4)	170.11(4)
Sr	z	0.3067(4)	0.3067(3)	0.3067(4)	0.3066(2)	0.3066(2)	0.3066(2)
Cu	z	0.1452(2)	0.1452(3)	0.1455(2)	0.1456(3)	0.1457(3)	0.1470(3)
O(1)	x	0.0390(1)	0.0390(2)	0.0390(2)	0.0390(2)	0.0390(1)	0.0390(2)
	z	0.3335(3)	0.3335(3)	0.3337(3)	0.3338(4)	0.3339(4)	0.3347(4)
O(2)	z	0.1295(1)	0.1295(2)	0.1297(4)	0.1295(3)	0.1295(3)	0.1295(4)
O(3)	x	0.1140(2)	0.1140(1)	0.1140(1)	0.1140(2)	0.1140(1)	0.1140(2)
Ru	N (Fe)	—	0.01(1)	0.04(2)	0.06(2)	0.07(1)	0.10(1)
Cu	N (Fe)	—	0.02(2)	0.01(3)	0.02(2)	0.03(2)	0.08(2)
	R_p (%)	5.5	6.0	5.9	5.3	5.9	5.4
	R_{wp} (%)	7.2	7.9	7.7	7.0	6.7	7.0
	R_{exp} (%)	5.5	6.4	6.0	5.4	6.3	5.7
	χ^2 (%)	1.7	1.5	1.6	1.7	1.5	1.5

of $SrRuO_3$ and $Sr_3(Ru, Cu)_2O_7$ secondary phases. As an example, we show in figure 2 the fitted pattern of the x-ray spectra for the undoped sample.

The structural parameters obtained from the Rietveld refinements are shown in table 1. The oxygen atoms localized in the SrO layer are denoted as O(1), those located in the CuO_2 layer as O(2) and those in the RuO_2 layer as O(3). N(Fe) represents the occupancy parameter for Fe at the Ru and Cu sites. From the refinement results it is clear that the Fe ions occupy both the Ru and Cu sites. The table shows the crystallographic parameter values for all the samples studied; the values determined for the undoped sample are in agreement with other published results [5, 10]. Figure 3 shows the lattice parameters and the cell volume of the samples as a function of iron content x. The a-axis shows a slight increase with increasing x, while the c-axis shows a significant decrease with x. The net result is a decrease in volume with increasing x.

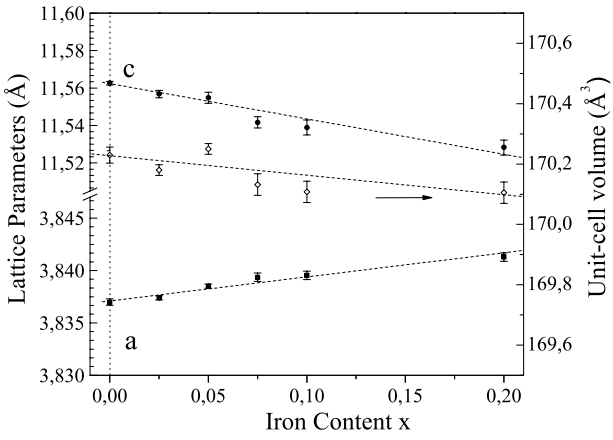

Figure 3. Crystal lattice parameters and unit cell volume as a function of Fe content x.

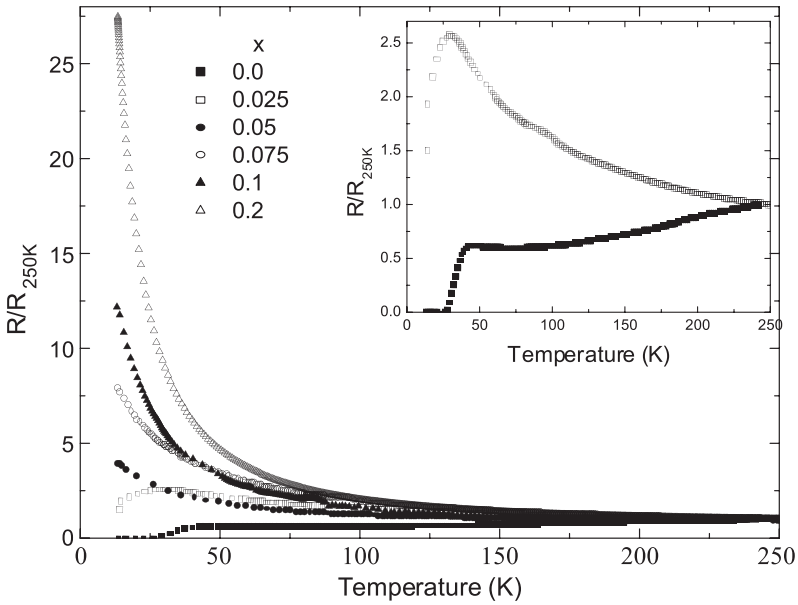

Figure 4. Normalized resistance as a function of temperature of the $Ru_{1-x}Fe_x$-1212 samples. The inset shows the curves for the $x = 0.0$ and 0.025 samples, where the superconducting transition is more clearly distinguished.

Table 2. Bond lengths (Å) and bond angles (deg) for $Ru_{1-x}Fe_x$-1212.

x	0.0	0.025	0.05	0.075	0.1	0.2
Bond lengths (Å)						
Ru–O(1)	1.931(4)	1.930(5)	1.927(3)	1.924(2)	1.923(3)	1.912(4)
Ru–O(3)	1.967(4)	1.968(5)	1.969(3)	1.969(5)	1.969(4)	1.970(4)
Cu–O(1)	2.182(4)	2.181(5)	2.180(3)	2.177(2)	2.177(3)	2.169(4)
Cu–O(2)	1.927(4)	1.927(5)	1.928(2)	1.929(3)	1.929(3)	1.931(4)
Bond angles (deg)						
Ru–O(3)–Ru	154.3(2)	154.3(3)	154.3(1)	154.3(2)	154.3(4)	154.3(2)
Cu–O(2)–Cu	169.2(2)	169.2(1)	169.1(3)	168.9(2)	168.8(2)	168.0(1)
ϕ (Cu–O(1)–Ru)	171.6(2)	171.6(2)	171.6(1)	171.5(2)	171.5(1)	171.5(2)

A list of the Rietveld-fitted bond lengths and bond angles for the samples is given in table 2. We observe that both the Ru(Fe)–O(1) and Cu(Fe)–O(1) bond lengths decrease with increasing Fe content and they should be associated with the shortening of the c axis.

The different characteristic angles of the structure show the following behaviours with increasing x. (a) The bond angle ϕ (Cu–O(1)–Ru), which is related to the deviation of the apical oxygen O(1) along the plane perpendicular to the c-axis, whose value determines the distortion of the RuO_6 octahedra, essential for the magnetic exchange interaction, shows no significant changes. (b) The bond angle Ru–O(3)–Ru, which is a measure of the rotation of the RuO_6 octahedra around the c-axis, remains constant. (c) The bond angle Cu–O(2)–Cu, which is a measure of the buckling of the CuO_2 layer, shows a slight tendency to decrease indicating an increase in the buckling of the CuO_2 layer.

Figure 4 shows the normalized resistance as a function of temperature for all samples investigated. The $R(T)$ curves for samples showing superconducting transitions are plotted in the inset of the figure. On decreasing the temperature, the resistance curve of the undoped sample shows a steady decrease until a relative minimum is attained around $T = 75$ K; then a slight increase is observed just before the onset of superconductivity at $T = 45$ K; the zero-resistance state is reached at $T = 25$ K. For the $x = 0.025$ sample, the $R(T)$ curve increases as the temperature decreases until it reaches the onset of the superconducting transition temperature at $T = 30$ K. For samples with $x \geqslant 0.05$, the $R(T)$ curves show a semiconducting-like temperature behaviour, without any signal of a superconducting transition, at least to the minimum temperature of 14 K investigated.

The superconducting transition temperature of the $Ru_{1-x}Fe_x$-1212 system drops quite fast with increase of the iron content and superconductivity is suppressed around 5% of Fe substitution. From the Rietveld refinement results, the Fe atoms partially substitute for Cu atoms in the CuO_2 layers, and many previous studies on high-T_c cuprate superconductors have shown that Fe substitution in CuO_2 layers rapidly degrades the superconducting state [22–25].

Furthermore, some studies have shown a correlation between the buckling of the CuO_2 layers and the superconducting transition temperature [26]. The highest T_c is achieved in structures with flat and square CuO_2 layers and long apical Cu–O bond lengths. In other words, an increase in the buckling of the CuO_2 layers and the shortening of the apical Cu–O bond lowers the transition temperature, due to a related hole localization phenomenon. Our Rietveld refinement

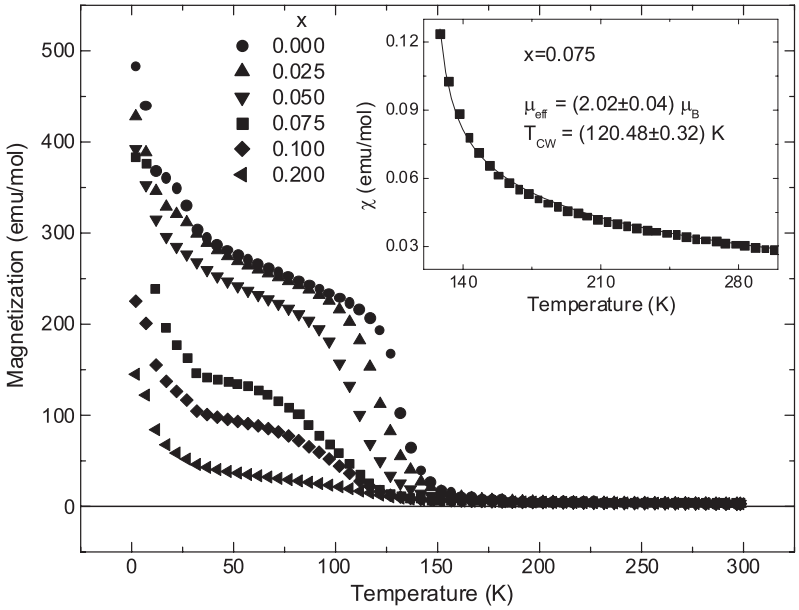

Figure 5. FC magnetization measurements as a function of temperature for the $Ru_{1-x}Fe_xSr_2GdCu_2O_8$ samples. The inset shows the Curie–Weiss fitting of the susceptibility data for the $x = 0.075$ sample. The indicated μ_{eff} and T_{CW} values correspond to the magnetic parameters of the Ru sublattice.

studies show that there is an increasing buckling tendency of the CuO_2 layer and a decreasing Cu–O(1) bond length with increase of the Fe content, resulting in a fast degradation of T_c and the ultimate disappearance of superconductivity.

Figure 5 shows the temperature dependence of the field cooled (FC) dc magnetization measurements, $M(T)$, obtained in an applied magnetic field $H_a = 100$ Oe. All samples show the characteristic ferromagnetic ordering transition curves and, in particular, the transition temperature for the undoped sample occurs at around $T = 140$ K. As the Fe content is increased, a broadening of the transition and a reduction of the magnetic ordering transition temperature are observed. An important result that can be derived from the Rietveld refinement of our x-ray data is that there are no significant changes in the bond angle ϕ, which is a measure of the canting of the Ru magnetic moment necessary to explain the appearance of ferromagnetism. Therefore, the above-mentioned magnetic behaviour is due not to a structural change, but to a weakening of the magnetic interaction between the Ru magnetic moments of the Ru sublattice. This behaviour was also observed when Ru was replaced by other elements [13–17]. At temperatures below 40 K the $M(T)$ curves show an increase due to the paramagnetic contribution of the Gd ions. The Gd sublattice remains in the paramagnetic state when the Ru sublattice is ordered ferromagnetically, and orders antiferromagnetically at $T_N = 2.8$ K [19]. However, it is worth noting that in a recent study, the possibility that the net ferromagnetic moment of the Ru sublattice can induce a small component of ferromagnetic ordering at the Gd sites that would contribute to the total magnetic moment of the system was found [27].

To determine the effect of Fe doping on the effective magnetic momenta, μ_{eff}, as well as on the magnetic ordering temperature of our samples, we fitted the magnetic susceptibility data, $\chi(T) = M(T)/H_a$, with the sum of two Curie–Weiss functions $\chi = C/(T - T_{CW})$, assuming

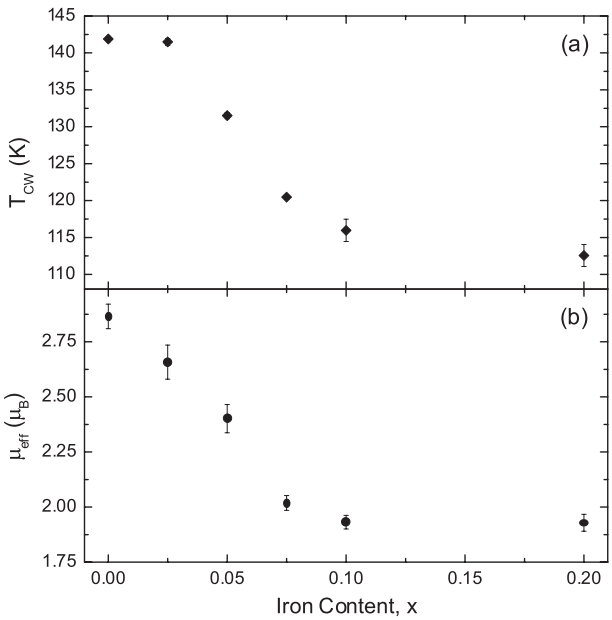

Figure 6. (a) Curie–Weiss temperature as a function of the Fe content x. (b) Effective magnetic moment as a function of the Fe content x.

independent contributions of the Gd and the Ru sublattices. The fitting was done in the 150–300 K temperature range. The magnetic parameters of the Gd ions were kept fixed at $\mu_{eff} = 7.94\ \mu_B$ and $T_{CW} = -4$ K values [19]. The effective magnetic moment was determined trough the relation $C = N\mu_{eff}^2/3k_B$ (N: Avogadro's number; k_B: Boltzmann's constant). As a representative fit, the inset of figure 5 shows, as a continuous line, the $\chi(T)$ of the sample for $x = 0.075$. The resulting fitting parameters for the Ru sublattice are given in table 3 and figure 6 shows the μ_{eff} and T_{CW} values as functions

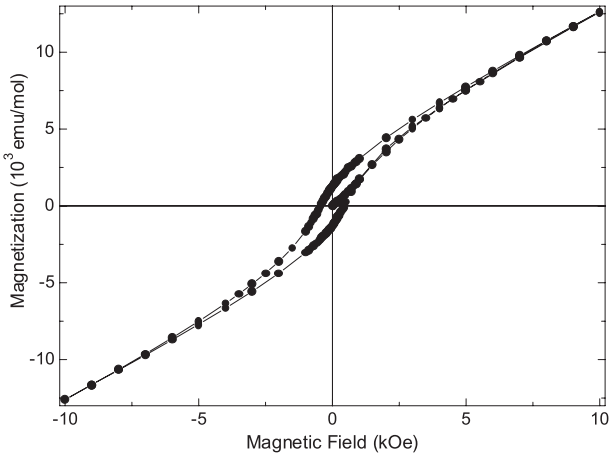

Figure 7. Hysteresis loop for a $Ru_{0.95}Fe_{0.05}Sr_2GdCu_2O_8$ sample, measured at 5 K.

Table 3. Parameters obtained from the temperature dependence of the magnetic susceptibility of $Ru_{1-x}Fe_x$-1212. C is the Curie–Weiss constant, T_{CW} is the Curie–Weiss temperature and μ_{eff} is the effective magnetic moment associated with Ru.

x	C (emu K mol^{-1})	T_{CW} (K)	μ_{eff} (μ_B)
0.0	1.03 ± 0.04	141.88 ± 0.37	2.87 ± 0.06
0.025	0.89 ± 0.05	141.49 ± 0.46	2.66 ± 0.08
0.050	0.72 ± 0.04	131.50 ± 0.42	2.40 ± 0.06
0.075	0.51 ± 0.02	120.48 ± 0.32	2.02 ± 0.03
0.10	0.45 ± 0.02	115.96 ± 1.51	1.93 ± 0.03
0.20	0.47 ± 0.02	112.56 ± 1.48	1.93 ± 0.04

of the Fe content. We observe that both μ_{eff} and T_{CW} decrease with increase of the Fe content, results that were expected from our analysis of the weakening of the magnetic interaction between the Ru moments provoked by Fe doping. The value of $\mu_{eff} = 2.87\ \mu_B$, obtained for $x = 0$, is in agreement with other reported values [16].

Magnetization measurements as a function of the applied magnetic field, below the magnetic transition temperatures, were also made. Before each measurement the sample was warmed above 150 K and cooled down in zero field. As an example, figure 7 shows the $M(H)$ hysteresis curve for the $x = 0.05$ sample, measured at $T = 5$ K, with the magnetic field changing between -10 kOe and +10 kOe. The magnetization curve shows the hysteresis loop of ferromagnetic materials although it displays a non-saturated characteristic due to the paramagnetic contribution of the Gd sublattice.

Finally we would like to point out that Mössbauer studies, currently in process, have shown no magnetic signals due to the presence of impurity phases detected in the x-ray spectra, so it must be concluded that the magnetic behaviour results obtained are only due to the Ru and Gd sublattices of the $Ru_{1-x}Fe_x$-1212 system. A detailed study will be published in the near future.

4. Conclusions

We have presented a study of the structural, superconducting and magnetic properties of the $Ru_{1-x}Fe_xSr_2GdCu_2O_8$ system. We found that the superconducting transition temperature T_c and the ferromagnetic transition temperature T_M both decrease with increase of the Fe content. The fast T_c decrement and the consequent quite fast disappearance of the superconducting state were explained by the fact that Fe ions not only occupy Ru sites but also Cu sites. It is well known that ion substitutions in the CuO_2 layers of high-T_c superconducting cuprates are a big source of T_c degradation. From the structural changes obtained, the shortening of the apical Cu–O bond length and a tendency of the CuO_2 layer to increase buckling with increasing Fe content could be associated with the observed T_c decrement. No significant changes were observed, with Fe doping, in the canting bond angle ϕ or in the RuO_6 octahedra rotation bond angle Ru–O(3)–Ru. Therefore the observed broadening of the transition and the reduction of the magnetic ordering temperature as the Fe content was increased are associated not with structural changes, but with a weakening of the magnetic interaction between the Ru moments of the Ru sublattice caused by doping.

Fitting two Curie–Weiss functions to the magnetic susceptibility data, assuming independent contributions of the Gd and the Ru sublattices, we quantify the effective magnetic momenta, μ_{eff}, of the Ru sublattice and the magnetic ordering temperature, T_{CW}, as a function of the Fe content.

Acknowledgment

The authors wish to acknowledge A Arevalo for his assistance in the preparation of the samples used in this work.

References

[1] Bauernfeind L, Widder W and Braun H F 1995 *Physica* C **254** 151
[2] Bauernfeind L, Widder W and Braun H F 1996 *J. Low. Temp. Phys.* **105** 1605
[3] Bernhard C, Tallon J L, Niedermayer Ch, Blasius Th, Golnik A, Brücher E, Kremer R K, Noakes D R, Stronach C E and Ansaldo E J 1999 *Phys. Rev.* B **59** 14099
[4] Pringle D J, Tallon J L, Walker B G and Trodahl H J 1999 *Phys. Rev.* B **59** R11679
[5] McLaughlin A C, Zhou W, Attfield J P, Fitch A N and Tallon J L 1999 *Phys. Rev.* B **60** 7512
[6] Felner I, Asaf U, Reich S and Tsabba Y 1999 *Physica* C **311** 163
[7] Klamut P W, Dabrowski B, Maxwel M, Mais J, Chmaissem O, Kruk R, Kmiec R and Kimball C W 2000 *Physica* C **341–348** 455
[8] Tallon J L, Loram J W, Williams G V M and Bernhard C 2000 *Phys. Rev.* B **61** R6471
[9] Bernhard C, Tallon J L, Brücher E and Kremer R K 2000 *Phys. Rev.* B **61** R14960
[10] Chmaissem O, Jorgensen J D, Shaked H, Dollar P and Tallon J L 2000 *Phys. Rev.* B **61** 6401
[11] Lynn J W, Keimer B, Ulrich C, Bernhard C and Tallon J L 2000 *Phys. Rev.* B **61** R14964
[12] Williams G V M and Krämer S 2000 *Phys. Rev.* B **62** 4132
[13] McLaughlin A C and Attfield J P 1999 *Phys. Rev.* B **60** 14605
[14] López A, Souza Azevedo I, Musa J E, Baggio-Saitovitch E and García García S 2003 *Phys. Rev.* B **68** 134516
[15] Malo S, Ko D, Rijssenbeek J T, Maignan A, Pelloquin D, Dravid V P and Poeppelmeier K R 2000 *Int. J. Inorg. Mater.* **2** 601
[16] Hassen A, Hemberger J, Loidl A and Krimmel A 2003 *Physica* C **400** 71

[17] Yang L T, Liang J K, Liu Q L, Song G B, Liu F S, Luo J and Rao G H 2004 *Physica* C **403** 177
[18] Klamut P W, Dabrowski B, Kolesnik S, Maxwell M and Mais J 2001 *Phys. Rev.* B **63** 224512
[19] Mandal P, Hassen A, Hemberger J, Krimmel A and Loidl A 2002 *Phys. Rev.* B **65** 144506
[20] Tallon J L, Loram J W, Williams G V M and Bernhard C 2000 *Phys. Rev.* B **61** R6471
[21] Hunter B A 1997 Rietica *IUCR Powder Diff.* **22** 21
[22] Maeno Y, Kato M, Aoki Y and Fujita T 1987 *Japan. J. Appl. Phys.* **26** L1982
[23] Yang C Y, Heald S M, Tranquada J M, Xu Y, Wang Y L, Moodenbaugh A R, Welch D O and Suenaga M 1989 *Phys. Rev.* B **39** 6681
[24] Akachi T, Escamilla R, Marquina V, Jiménez M, Marquina M L, Gómez R, Ridaura R and Aburto S 1998 *Physica* C **301** 315
[25] Escamilla R, Akachi T, Gómez R, Marquina V, Marquina M L and Ridaura R 2002 *Supercond. Sci. Technol.* **15** 1074
[26] Kambe S and Ishii O 2000 *Physica* C **341–348** 555
[27] Jorgensen J D, Chmaissem O, Shaked H, Short S, Klamut P W, Dabrowski B and Tallon J L 2001 *Phys. Rev.* B **63** 054440